

Observability-Aware Control for Cooperatively Localizing Quadrotor UAVs

H S Helson Go¹ Ching Lok Chong² Longhao Qian¹ Hugh H.-T. Liu¹

Abstract—Cooperatively Localizing robots should seek optimal control strategies to maximize precision of position estimation and ensure safety in flight. Observability-Aware Trajectory Optimization has strong potential to address this issue, but no concrete link between observability and precision has been proven yet. In this paper, we prove that improvement in positioning precision inherently follows from optimizing observability. Based on this finding, we develop an Observability-Aware Control principle to generate observability-optimal control strategies. We implement this principle in a Model Predictive Control framework, and we verify it on a team of quadrotor Unmanned Aerial Vehicles comprising a follower vehicle localizing itself by tracking a leader vehicle in both simulations and real-world flight tests. Our results demonstrate that maximizing observability contributed to improving global positioning precision for the quadrotor team.

SUPPLEMENTARY MATERIALS

We open-source two pieces of software used in this work: Our observability-aware controller at https://github.com/FSC_Lab/observability_aware_controller, and our UWB ranging system at https://github.com/FSC_Lab/dwm3000_ros.

I. INTRODUCTION

Multi-Robot Systems may employ Cooperative Localization (CL) in exploration [1]–[3] and navigating in spite of flaws in Global Navigation Satellite Systems (GNSS) [4]–[6]. A team of robots achieve CL by sharing sensor data, measuring some aspects of interrobot pose, and fusing these data in a state estimator to jointly estimate their states.

In practice, simple interrobot sensors on small robots like micro quadrotors cannot directly observe every component of system state. In the scenario of a leader-follower robot team, even if the follower can measure its range — in one dimension — to the leader, it cannot deduce all 3 coordinates of its position relative to the leader. Thus, it must take observations along specific trajectories to regain full state information and thereby navigate safely. Generalizing this problem, designing a trajectory to enhance observability is called *Observability-Aware Trajectory Optimization*.

Observability reflects the ability of a dynamical system to determine its states given observations along its trajectory. Recent works proposed trajectory optimization metrics based on the Local Observability Gramian, which is variously approximated by numerical means [7] or by Taylor expansions

H S Helson Go, Longhao Qian, and Hugh H.-T. Liu are with the Institute for Aerospace Studies, University of Toronto (UTIAS), 4925 Dufferin Street, Toronto, Canada hei.go@mail.utoronto.ca, longhao.qian@mail.utoronto.ca hugh.liu@utoronto.ca

² Ching Lok Chong is a graduate of Oxford University, OCIAM, now working in quantitative finance.

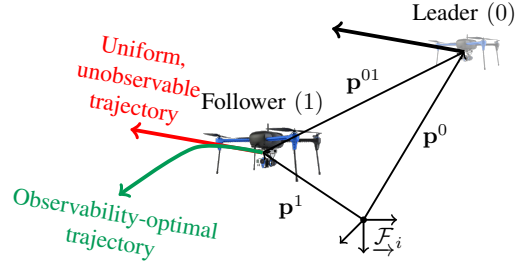


Fig. 1. Visualizing a Cooperative Localization System with a leader and a follower. The leader’s position p^0 is directly measured but that of the followers p^1 must be indirectly measured. Only the interrobot range ($\dim = 1$) instead of the full interrobot positions ($\dim 3$) is measured so a special trajectory (green path) is needed to recover information on the state.

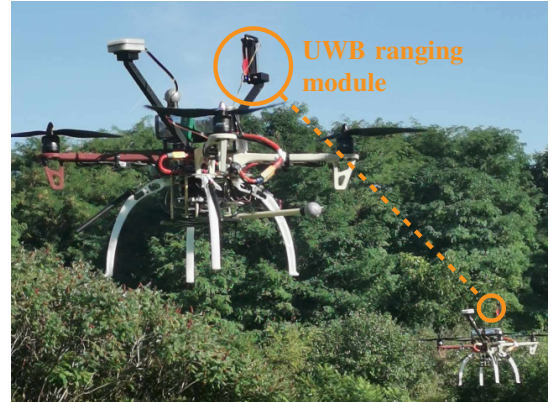


Fig. 2. A practical cooperative localization system based on Ultra-Wideband (UWB) interrobot ranging mounted on a pair of F450 quadrotors, portrayed in flight during our flight test experiments

of the underlying system dynamics [8]–[10]. It has been shown that observability-optimal trajectories let a system avoid configurations where a part of the states become unobservable. Although this approach is applied to sensor self-calibration in most existing works, it is a strong candidate to address the issue of observing the full system state by dimensionally-deficient observations in CL.

Before adopting observability-aware trajectory optimization, this approach’s relationship with *uncertainty-aware trajectory optimization* must be addressed. The latter is well established in the area of robot CL since it is a natural extension to the Extended Kalman Filter (EKF) on CL systems. It seeks trajectories that minimize some metric of the EKF covariance matrix [11]–[13].

An earlier body of work [14], [15] linked the Observability Gramian to bounds on EKF covariance. However, these conclusions do not necessarily imply that optimizing aspects of the observability has any positive impact on covariance.

Another open question is whether observability-optimal trajectories satisfy *local weak observability* [16] that is directly evolved from the classical definition of observability of linear systems. To our best knowledge, no work proved this beyond empirically demonstrating that observability-optimal trajectories avoid unobservable configurations.

In this paper, we present an optimal control problem based on maximizing observability through a novel approximation of the Observability Gramian. Our formulation is informed by our derivation of the intrinsic link between observability maximization and positioning uncertainty reduction.

We solve this problem in a receding-horizon framework to give us the Observability Predictive Controller (OPC), which complies with the Model Predictive Controller (MPC) formalism and inherits its applicability to both real-time control and offline trajectory generation. We also prove that the solution to this problem satisfies classical observability rank conditions.

To verify our framework, we consider a leader-follower team of quadrotors. Only the leader is equipped with GNSS, and the follower must cooperatively localize itself by measuring its distance to the leader. By design, the observations do not cover the state space so an observability-optimal control solution is necessary to observe the full state.

We use this configuration in simulations to demonstrate that positioning uncertainty is minimized along observability-optimal trajectories, and then we apply this configuration when flight testing a team of quadrotor platforms shown in Figure 2.

In summary, our contributions in this paper are

- We derive the Short-Term Local Observability Gramian (STLOG), a novel approximation of the Local Observability Gramian
- We propose the Observability-Aware Control principle, an optimal control law that maximizes precision improvement

II. RELATED WORK

A well established problem in Cooperative Localization is finding optimal motion strategies that let cooperatively localizing robots maximize various performance metrics such as inter-robot connectivity [17], amount of information [18], positioning precision [11]–[13] and observability.

Precision maximization attracted early attention since precision is intuitively understood and conventional EKF-based state estimators on CL systems readily track the evolution of estimation covariance (inverse of precision).

Under the paradigm of covariance-aware trajectory optimization, Trawny and Barfoot [11] chose the logarithm of the determinant of the EKF covariance matrix as the objective to compute the optimal trajectory. Despite obtaining encouraging numerical results showing improved localization precision when robots follow optimized trajectories, they reported significant issues with the EKF approach that is not fully addressed in successive works over the years.

Firstly, recursively evaluating the EKF prediction and update equations to compute the covariance matrix amounts to numerical integration. This leads to an objective function that is nonconvex and subtly discontinuous, hindering most gradient-based solvers. Later works variously addressed this issue by adopting the Genetic Algorithm as the solver [12] and optimizing over a single timestep so that the minima of the objective function can be analytically found [13].

Secondly, Trawny chose to propagate the EKF state by ideal system dynamics without simulating noise, essentially propagating covariance along noiseless trajectories. The authors questioned this practice themselves as the EKF covariance propagation equations are founded on the assumption that system inputs and observations are affected by zero-mean Gaussian noise. So far, only our previous work [19] attempted to verify if the Kalman-based objective accurately represents the estimation uncertainty in the presence of noise.

Although observability-aware trajectory optimization has only recently been considered in the area of CL, observability analysis is already ubiquitous here, especially in works exploring CL of Unmanned Aerial Vehicles (UAVs) [20]–[22]. These works used Hermann and Krener’s observability rank condition [16] to test the observability of CL systems in various configurations. The observability rank condition is *binary*, and it is soon complemented by Krener and Ide [7]’s *Empirical Local Observability Gramian (ELOG)* matrix, which is a numerical approximation of the Observability Gramian [23] and whose smallest singular value offers a measure of observability. Nevertheless, evaluating the ELOG involves numerically integrating system dynamics, making it susceptible to the same issues that affect covariance-based objectives.

Observability-aware trajectory optimization saw practical application in the fields of landmark-based localization [24] and sensor self-calibration [8]–[10]. In particular, Hausman, Priess, *et al.* [8] introduced the *Expanded Empirical Local Observability Matrix (E²LOG)*, which relies on a Taylor expansion of the sensor model that can be expressed as Lie Derivatives of the latter, to approximate the Observability Gramian. The E²LOG can be expressed analytically in terms of system dynamics and observation models and their derivatives, making for a computationally efficient implementation. Grebe *et al.* [10] carried out a comparative study of trajectory optimization based on the E²LOG and a closely-related alternative method based on information filtering [24], revealing the quantitative benefit of observability-based techniques.

Only very recently did the adoption of observability-aware trajectory optimization spread to the area of CL of UAVs. Boyinine *et al.* [25] suggested an observability-aware path planner that minimizes the trace of the observability Gramian. However, this work considered planar robots, whose simple system dynamics enabled researchers to derive the underlying observability Gramian symbolically and simplify its expression by manual inspection.

Building on these works, there is yet room for innovating new means of approximating the Local Observability Gramian for optimization purposes. More fundamentally, whether observability maximization contributes to covariance minimization is yet to be answered.

III. PROBLEM STATEMENT

A. Notation

We use lowercase a for scalars, lowercase bold \mathbf{a} for vectors (column-matrices) and uppercase bold \mathbf{A} for matrices.

We use a functional notation scheme. We denote composition of two functions by \circ , such that $f \circ g = f(g(\dots))$. For functions that take functions as arguments, we use the arrow notation, e.g. $g(f : \mathcal{X} \rightarrow \mathcal{Y})$ to identify functional arguments. For a unary function g , we denote its derivative by Dg and its r^{th} -order Lie derivative along a vector field \mathbf{f} by $L_{\mathbf{f}}^{(r)}g$.

We use unit quaternions $\mathbf{q} \in S^3$ to represent quadrotor attitude, specifically the rotation of the inertial frame relative to the quadrotor body frame. We denote the quaternion product by the \otimes operator, the conversion of a quaternion to its equivalent rotation matrix by $\mathbf{R}(\mathbf{q})$, and forming a purely imaginary quaternion from a 3-vector by $\mathcal{I}^*(\mathbf{v}) \triangleq [\mathbf{v}^\top \ 0]^\top$.

Furthermore, we equip all vector spaces with the standard Euclidean inner product $\langle \mathbf{u}, \mathbf{v} \rangle = \mathbf{u}^\top \mathbf{v}$ with corresponding norm $\|\cdot\|$.

B. Model of Cooperatively Localizing Quadrotors

We consider a system of N quadrotors with a leader-follower topology. Let each quadrotor's state be $\mathbf{x}^i = (\mathbf{p}^i, \mathbf{q}^i, \mathbf{v}^i)$, respectively its position, attitude and velocity in the inertial frame. Let the control input to each quadrotor be $\mathbf{u}^i = (f^i, \boldsymbol{\omega}^i)$, respectively the thrust-per-unit-mass delivered along the quadrotor's body z-axis, and the angular velocity. With these definitions, our state space is $\mathcal{X} \subset \mathbb{R}^{10}$ and input space is $\mathcal{U} \subset \mathbb{R}^4$, and the motion model of each quadrotor is

$$\dot{\mathbf{x}}^i = \mathbf{f}(\mathbf{x}^i, \mathbf{u}^i) \triangleq \begin{bmatrix} \mathbf{v}^i \\ \mathbf{q}^i \otimes \mathcal{I}^*(\boldsymbol{\omega}^i) \\ f^i \mathbf{R}(\mathbf{q}^i) \mathbf{1}_3 + \mathbf{g} \end{bmatrix}, \quad (1)$$

where $\mathbf{g} = [0 \ 0 \ -9.81]^\top$ is the gravity vector.

We adopt a centralized architecture for the system of quadrotors. Hence, the entire system state is given by $\mathbf{x} = (\mathbf{x}^1, \dots, \mathbf{x}^N)$, the corresponding control inputs by $\mathbf{u} = (\mathbf{u}^1, \dots, \mathbf{u}^N)$, and the system motion model by

$$\mathbf{f}(\mathbf{x}, \mathbf{u}) = \begin{bmatrix} \mathbf{f}(\mathbf{x}^0, \mathbf{u}^0) \\ \vdots \\ \mathbf{f}(\mathbf{x}^N, \mathbf{u}^N) \end{bmatrix} \quad (2)$$

We consider four sources of information in the observation model. Firstly, the leader directly observes its absolute position through GNSS. The position observation model is simply

$$\mathbf{h}^{\text{pos}}(\mathbf{x}) \triangleq \mathbf{p}^0 \quad (3)$$

To localize themselves, each follower tracks the range of the leader quadrotor from itself. The one-dimensional range observation model is given by

$$\mathbf{h}^{0i}(\mathbf{x}) \triangleq \rho^{0i} = \|\mathbf{p}^0 - \mathbf{p}^i\| \quad (4)$$

For brevity, we assume each quadrotor can directly observe its attitude and velocity through modern AHRS or odometry systems. Their observation models are

$$\mathbf{h}^{\text{vel}}(\mathbf{x}) \triangleq \begin{bmatrix} \mathbf{v}^1^\top & \dots & \mathbf{v}^N^\top \end{bmatrix} \quad (5)$$

$$\mathbf{h}^{\text{att}}(\mathbf{x}) \triangleq \begin{bmatrix} \mathbf{q}^1^\top & \dots & \mathbf{q}^N^\top \end{bmatrix} \quad (6)$$

Our system's state space has dimension $10N$, but its observation space only has dimension $2 + 8N$, resulting in an unobservable subspace of dimension $2N - 2$, greater than 0 for all $N \geq 2$. Even so, full position information is observable to the follower if it adopts a beneficial motion strategy. Generating such a strategy is the problem to be tackled by this paper, with the approach of designing a trajectory optimization problem and solving it.

IV. OBSERVABILITY

In this section, we review notions of observability in the literature, including the Observability Gramian. Then we apply Bayesian inference to prove the link between observability maximization and covariance minimization. Finally, we introduce the *short-time local observability Gramian*.

A. Observability Analysis

We investigate observability in the context of the nonlinear dynamical system

$$S : \begin{cases} \dot{\mathbf{x}} = \mathbf{f}(\mathbf{x}, \mathbf{u}), & \mathbf{x}(t=0) = \mathbf{x}_0 \\ \mathbf{y} = \mathbf{h}(\mathbf{x}) + \boldsymbol{\eta}, \end{cases} \quad (7)$$

with state space $\mathcal{X} \subset \mathbb{R}^n$, input space $\mathcal{U} \subset \mathbb{R}^m$ and observation space $\mathcal{Y} \subset \mathbb{R}^p$.

Furthermore, let $\phi_t : \mathcal{X} \rightarrow \mathcal{X}$ be the deterministic flow of \mathbf{f} for inputs $\mathbf{u}(t)$.¹ In other words, $\mathbf{x}(t) = \phi_t(\mathbf{x}_0)$ is the unique solution to $\dot{\mathbf{x}} = \mathbf{f}(\mathbf{x}, \mathbf{u})$ for each initial condition \mathbf{x}_0 .

A textbook [23] definition for observability is that a system is observable if and only if the *Observability Gramian*

$$\mathbf{W} = \int_0^T \boldsymbol{\Phi}_t^\top \mathbf{H}^\top \mathbf{H} \boldsymbol{\Phi}_t dt, \quad (8)$$

is nonsingular. For a nonlinear system such as (7), the state transition matrix $\boldsymbol{\Phi}_t$ and observation matrix \mathbf{H} in (8) are obtained by linearizing about an operating point such that $\boldsymbol{\Phi}_t = D\phi_t$ and $\mathbf{H} = D\mathbf{h}$, and (8) is referred to in a qualified sense as the *Local Observability Gramian* [7]. However, this matrix is generally approximated since closed-form expressions for ϕ_t and hence $\boldsymbol{\Phi}_t$ are unavailable

In practice, Hermann and Krener's [16] *rank test* instead of the textbook definition is used to detect the observability of a dynamical system. In the test, the Observability Matrix

$$\mathcal{O}^{(r)}(\mathbf{x}, \mathbf{u}) = \begin{bmatrix} D\mathbf{h} \\ DL_{\mathbf{f}}\mathbf{h} \\ \vdots \\ DL_{\mathbf{f}}^r\mathbf{h} \end{bmatrix}, \quad (9)$$

¹This flow ϕ_t is time-dependent since the vector field $\mathbf{f}(\mathbf{x}, \mathbf{u})$ has an explicit time dependence through the inputs $\mathbf{u}(t)$. Moreover, $\phi_t[\mathbf{u}(t)]$ depends on the inputs $\mathbf{u}(t)$ as a *functional*. We suppress this functional dependence throughout and only emphasize it when necessary.

is formed. The system is said to be *weakly locally observable* at (\mathbf{x}, \mathbf{u}) if $\text{rank } \mathcal{O}^{(r)}(\mathbf{x}, \mathbf{u}) = \dim \mathcal{X}$ for some r .

The above procedure tests if a system are observable or not at an operating point in a binary sense. As for metrics of observability, the minimum singular value [7]–[9] and the trace [25] of the Local Observability Gramian have been used variously.

To prepare us for reconciling the binary notion and metric of observability, we define the *local observability index*

$$r_*(\mathbf{x}, \mathbf{u}) = \inf \left\{ r \mid \text{rank } \mathcal{O}^{(r)}(\mathbf{x}, \mathbf{u}) = \dim \mathcal{X} \right\}, \quad (10)$$

which is the minimum order of Lie derivatives r necessary for observability matrix to attain a rank equal to $\dim \mathcal{X}$.

This is a discrete metric of observability. Low $r_*(\mathbf{x}, \mathbf{u})$ corresponds to high observability and vice versa. At one extreme, the system is unobservable when $r_*(\mathbf{x}, \mathbf{u})$ is infinite. Thus, the binary notion of weak local observability is recovered from the finiteness of r_* .

B. The Observability Gramian from initial condition estimation

To build the link between observability theory and state estimation, we focus on problems where

- 1) the initial condition \mathbf{x}_0 is uncertain and modeled as a normally distributed random variable defined by a known mean and covariance $\mathbf{x}_0 \sim \mathcal{N}(\mathbf{x}_0^*, \check{\mathbf{P}}_0)$;
- 2) there is no process noise i.e. the evolution is deterministic; and
- 3) the observation noise $\boldsymbol{\eta}$ is i.i.d. and follows a normal distribution $\boldsymbol{\eta} \sim \mathcal{N}(0, \mathbf{R})$.

We seek to improve our estimate for \mathbf{x}_0 given future observations $\mathbf{y}(t)$ in the horizon $[0, T]$. Said improvement is embodied by the posterior distribution of the initial condition, written as $p(\mathbf{x}_0 | t \mapsto \mathbf{y}(t))$, where $t \mapsto \mathbf{y}(t)$ denotes the observation model evaluated in regular intervals of Δt to yield the observations $\mathbf{y}(t_0, \dots, t_{n-1})$ where $n = T/\Delta t$.

Firstly, we factor this distribution by Bayes' rule

$$p(\mathbf{x}_0 | t \mapsto \mathbf{y}(t)) = C p(t \mapsto \mathbf{y}(t) | \mathbf{x}_0) p(\mathbf{x}_0), \quad (11)$$

where C is a normalization constant independent of \mathbf{x}_0 .

Then, we compute the likelihood $p(t \mapsto \mathbf{y}(t) | \mathbf{x}_0)$. When the initial condition \mathbf{x}_0 is given, each $\mathbf{y}(t_i)$ is normally distributed with mean $\mathbf{h}(\phi_{t_i}(\mathbf{x}_0))$ and covariance \mathbf{R} due to the deterministic evolution, and are pairwise independent.

Hence, we denote the map that sends the initial condition \mathbf{x}_0 to the expected observation $\mathbf{h}(\mathbf{x}(t))$ at time t by

$$\mathcal{A}_t : \mathcal{X} \rightarrow \mathcal{Y}, \quad \mathcal{A}_t(\mathbf{x}_0) = \mathbf{h}(\phi_t(\mathbf{x}_0)), \quad (12)$$

Defining the residual between expected and actual observations as

$$\mathbf{z}_t = \mathbf{y}(t) - \mathcal{A}_t(\mathbf{x}_0), \quad (13)$$

we can write the likelihood $p(t \mapsto \mathbf{y}(t) | \mathbf{x}_0)$ as

$$\begin{aligned} p(t \mapsto \mathbf{y}(t) | \mathbf{x}_0) &= \sum_{i=0}^{n-1} p(\mathbf{y}(t_i) | \mathbf{x}_0) \\ &= C \prod_{i=0}^{n-1} \exp \left(-\frac{1}{2} \mathbf{z}_{t_i}^\top \mathbf{R}^{-1} \mathbf{z}_{t_i} \right) \\ &= C \exp \left(\sum_{i=0}^{n-1} -\frac{1}{2} \mathbf{z}_{t_i}^\top \mathbf{R}^{-1} \mathbf{z}_{t_i} \right) \\ &\simeq C \exp \left(-\frac{1}{2} \frac{1}{\Delta t} \int_0^T \mathbf{z}_t^\top \mathbf{R}^{-1} \mathbf{z}_t dt \right). \end{aligned} \quad (14)$$

Substituting Equation (14) into (11) gives a full description of the posterior $p(\mathbf{x}_0 | t \mapsto \mathbf{y}(t))$.

To obtain more relevant analytical results, let us assume that the prior covariance is small $\|\check{\mathbf{P}}_0\| \ll 1$, and that the probability density of any \mathbf{x}_0 far away from the prior mean \mathbf{x}_0^* is negligible.

We denote the variations of the random state and observation from their respective means by

$$\begin{aligned} \delta \mathbf{x}_0 &= \mathbf{x}_0 - \mathbf{x}_0^*, \\ \delta \mathbf{y}(t) &\triangleq \mathbf{y}(t) - \mathbf{y}^*(t) \text{ where } \mathbf{y}^*(t) \triangleq \mathcal{A}_t(\mathbf{x}_0^*). \end{aligned}$$

This allows us to expand the residual (13) for small $\delta \mathbf{x}_0$, giving

$$\mathbf{z}_t = \mathbf{y}(t) - \mathcal{A}_t(\mathbf{x}_0) \simeq \delta \mathbf{y}(t) - D\mathcal{A}_t \delta \mathbf{x}_0, \quad (15)$$

which allows us to simplify the likelihood (14) as

$$\begin{aligned} p(t \mapsto \delta \mathbf{y}(t) | \delta \mathbf{x}_0) \\ = C \exp \left(-\frac{1}{2} \frac{1}{\Delta t} \delta \mathbf{x}_0^\top \mathbf{W}_{\mathbf{R}^{-1}} \delta \mathbf{x}_0 + \frac{1}{\Delta t} \delta \mathbf{x}_0^\top \mathbf{b} \right), \end{aligned} \quad (16)$$

where

$$\mathbf{W}_{\mathbf{R}^{-1}} = \int_0^T D\mathcal{A}_t^\top \mathbf{R}^{-1} D\mathcal{A}_t dt, \quad (17)$$

$$\mathbf{b} = \int_0^T D\mathcal{A}_t^\top \mathbf{R}^{-1} \delta \mathbf{y}(t) dt. \quad (18)$$

The matrix $\mathbf{W}_{\mathbf{R}^{-1}}$ is known as the *Observability Gramian* w.r.t. the metric \mathbf{R}^{-1} on the observation space \mathcal{Y} . If we take $\mathbf{R} = \mathbf{I}$ and note that $\mathcal{A}_t = \mathbf{h} \circ \phi_t$ and $D\mathcal{A}_t = \mathbf{H}\Phi_t$, then Equation (17) matches the traditional definition of the Gramian (8).

Under these approximations, Bayes' rule (11) gives the conditional distribution $\delta \mathbf{x}_0 | t \mapsto \mathbf{y}(t)$ as

$$\begin{aligned} p(\delta \mathbf{x}_0 | t \mapsto \mathbf{y}(t)) &= C p(t \mapsto \mathbf{y}(t) | \mathbf{x}_0) p(\mathbf{x}_0), \\ &= C \exp \left(-\frac{1}{2} \delta \mathbf{x}_0^\top \left(\frac{1}{\Delta t} \mathbf{W}_{\mathbf{R}^{-1}} + \check{\mathbf{P}}_0^{-1} \right) \delta \mathbf{x}_0 + \frac{\delta \mathbf{x}_0^\top \mathbf{b}}{\Delta t} \right), \end{aligned} \quad (19)$$

which is a normally distributed random variable with expectation and covariance

$$\mathbb{V}[\delta \mathbf{x}_0 | t \mapsto \mathbf{y}(t)] = \left(\frac{1}{\Delta t} \mathbf{W}_{\mathbf{R}^{-1}} + \check{\mathbf{P}}_0^{-1} \right)^{-1}, \quad (20)$$

$$E[\delta \mathbf{x}_0 | t \mapsto \mathbf{y}(t)] = \mathbb{V}[\delta \mathbf{x}_0 | t \mapsto \mathbf{y}(t)] \left(\frac{1}{\Delta t} \mathbf{b} \right). \quad (21)$$

We collect these results in a proposition:

Proposition IV.1. *Let $\mathbf{x}_0 \sim \mathcal{N}(\mathbf{x}_0^*, \check{\mathbf{P}}_0)$ be an uncertain initial condition for the dynamics (7). After n observations $t \mapsto \mathbf{y}(t)$ of the linearized dynamics around \mathbf{x}_0^* , the posterior distribution of \mathbf{x}_0 is $\mathcal{N}(\hat{\mathbf{x}}_0, \hat{\mathbf{P}}_0)$, where*

$$\hat{\mathbf{x}}_0 = \mathbf{x}_0^* + \frac{1}{\Delta t} \hat{\mathbf{P}}_0 \mathbf{b}, \quad (22)$$

$$\hat{\mathbf{P}}_0^{-1} = \frac{1}{\Delta t} \mathbf{W}_{\mathbf{R}^{-1}} + \check{\mathbf{P}}_0^{-1}. \quad (23)$$

The expressions for $\mathbf{W}_{\mathbf{R}^{-1}}$ and \mathbf{b} given in (17), (18) respectively, and Δt is the time interval between observations.

In particular, the minimum precision (inverse covariance) of the posterior distribution satisfies the following lower bound:

$$\lambda_{\max}(\hat{\mathbf{P}}_0)^{-1} \geq \frac{\lambda_{\min}(\mathbf{W}_{\mathbf{R}^{-1}})}{\Delta t} + \lambda_{\max}(\check{\mathbf{P}}_0)^{-1}, \quad (24)$$

where $\lambda_{\min/\max}$ denotes the minimum/maximum eigenvalue of the relevant matrix.

In other words, the minimum eigenvalue of the Local Observability Gramian provides a lower bound to the improvement in the precision of the initial condition estimate due to observations.

C. Short-term local observability Gramian

In this section we propose the *short-term local observability Gramian (STLOG)*, a novel closed-form approximation of the Observability Gramian, under the following conditions:

- 1) the observation horizon $T = n\Delta t$ is short, satisfying the ordering $\Delta t \lesssim T \ll 1$;
- 2) the input $\mathbf{u}(t)$ is constant for $t \in [0, T)$. Our dynamics (7) is therefore autonomous in this horizon $[0, T)$, with constant input \mathbf{u} .

Firstly, we expand the map \mathcal{A}_t (12) as a Taylor series in t about $t = 0$. Since $\mathcal{A}_t = \mathbf{h} \circ \phi_t$, we have

$$\mathcal{A}_t(\mathbf{x}_0) = \mathbf{h}(\mathbf{x}(t)). \quad (25)$$

Differentiating both sides of (25) w.r.t. t gives

$$\frac{d}{dt} \mathcal{A}_t(\mathbf{x}_0) = (L_{\mathbf{f}} \mathbf{h})(\mathbf{x}(t)), \quad (26)$$

where $L_{\mathbf{f}} = \mathbf{f} \cdot \nabla$ is the Lie derivative on functions².

For assumed constant inputs \mathbf{u} , \mathbf{f} has no explicit time-dependence, so the higher order time derivatives of (26) are

$$\frac{d^j}{dt^j} \mathcal{A}_t(\mathbf{x}_0) = \left(L_{\mathbf{f}}^j \mathbf{h} \right)(\mathbf{x}(t)), \quad (27)$$

evaluating each of which at $t = 0$ gives the Taylor series

$$\mathcal{A}_t(\mathbf{x}_0) = \sum_{j=0}^{\infty} \frac{t^j}{j!} \left(L_{\mathbf{f}}^j \mathbf{h} \right)(\mathbf{x}_0), \quad (28)$$

²This is consistent with the definition of Lie derivatives in differential geometry (see, e.g. [26]) if we consider \mathbf{h} as a p -tuple of scalar functions on the manifold \mathcal{X} , whence no contractions involving $D\mathbf{f}$ are necessary.

Note however that $D\mathbf{h}$ is considered as a p -tuple of one-forms on \mathcal{X} , and correspondingly $L_{\mathbf{f}} D\mathbf{h} = \mathbf{f} \cdot \nabla(D\mathbf{h}) + (D\mathbf{h})(D\mathbf{f})$. The usual identity $L_{\mathbf{f}} D\mathbf{h} = DL_{\mathbf{f}} \mathbf{h}$ holds under this interpretation.

which can be differentiated to give

$$D\mathcal{A}_t = \sum_{j=0}^{\infty} \frac{t^j}{j!} D \left(L_{\mathbf{f}}^j \mathbf{h} \right). \quad (29)$$

Substituting the series (29) into the Gramian (17) and integrating yields the following closed-form approximation:

Definition IV.1. The order- r *short-term local observability Gramian (STLOG)* is the matrix

$$\mathbf{W}_{\mathbf{R}^{-1}}^{(r)} = \sum_{i,j=0}^r \frac{T^{i+j+1}}{(i+j+1)i!j!} D(L_{\mathbf{f}}^i \mathbf{h})^{\top} \mathbf{R}^{-1} D \left(L_{\mathbf{f}}^j \mathbf{h} \right). \quad (30)$$

which would be evaluated at $(\mathbf{x}^*, \mathbf{u}; T)$, respectively the initial condition, control input, and the observation time.

In principle, the Lie-derivatives inside (30) are composed of expressions of \mathbf{f} , \mathbf{h} , and their derivatives. If analytical expressions of the latter are available, then (30) can be evaluated analytically.

Remark. The truncated forms of the Taylor expansions found in (28) and (29) have appeared in the observability literature.

- 1) For a generic initial condition \mathbf{x} , the Taylor series (29) truncated at order r can be written as

$$D\mathcal{A}_t = [\mathbf{1} \quad t\mathbf{1} \quad \cdots \quad \frac{t^r}{r!} \mathbf{1}] \mathcal{O}^{(r)}(\mathbf{x}(t), \mathbf{u}(t)), \quad (31)$$

where $\mathcal{O}^{(r)}(\mathbf{x}, \mathbf{u})$ is the *observability matrix* used in rank testing per (9).

- 2) Consider the dynamics from time t onwards with given initial condition $\mathbf{x}(t)$. Hausman, Priess, *et al.* [8] denotes the product between the two block matrices in (31) as

$$\mathbf{K}(t, \Delta t) \triangleq [\mathbf{1} \quad \Delta t \mathbf{1} \quad \cdots \quad \frac{\Delta t^r}{r!} \mathbf{1}] \mathcal{O}^{(r)}(\mathbf{x}(t), \mathbf{u}(t)),$$

and defines the following *Expanded Empirical Local Observability Gramian (E²LOG)*:

$$\mathbf{W}_{E^2LOG}(T, \Delta t) \triangleq \int_0^T \mathbf{K}(t, \Delta t)^{\top} \mathbf{K}(t, \Delta t) dt, \quad (32)$$

which is proposed as a measure of observability. However, the expression (32) converges to $\int_0^T D\mathbf{h}^{\top} D\mathbf{h} dt$ as $\Delta t \rightarrow 0$, which differs from the true Gramian (17) by factors of Φ_t in the integrand. This difference manifests as the observation/planning horizon T increases. Thus, in a trajectory optimization setting, there exist conditions where the E²LOG may deviate substantially from the Observability Gramian.

V. OBSERVABILITY-AWARE CONTROL

For control systems, we are interested in state estimates of $\mathbf{x}(t)$ at any operating point, instead of solely the initial condition treated in the previous section. In this section, we derive an optimal control law that yields an observability-optimal trajectory by maximizing the average precision gain from observations, embodied by the STLOG (IV.1).

We linearize our analysis around a true path $\mathbf{x}^*(t) = \phi_t(\mathbf{x}_0^*)$ and use the notation $\delta \mathbf{x}_t = \mathbf{x}(t) - \mathbf{x}^*(t)$. We relax the shortness requirement on the observation horizon T , but divide it into

N stages of size ΔT , so that $T = N\Delta T$ and stage- k starts at $T_k = k\Delta T$. Furthermore, we explicitly track the state expectations and covariance at each T_k . The observation period remains Δt , where $\Delta t \lesssim \Delta T \ll T$.

At each T_k , we introduce the conditional covariances:

$$\check{\mathbf{P}}_{T_k} = \mathbb{V}[\delta \mathbf{x}_{T_k} | \mathbf{y} : [0, T_k] \rightarrow \mathcal{Y}], \quad (33)$$

$$\hat{\mathbf{P}}_{T_k} = \mathbb{V}[\delta \mathbf{x}_{T_k} | \mathbf{y} : [0, T_{k+1}] \rightarrow \mathcal{Y}], \quad (34)$$

where $\check{\mathbf{P}}_{T_k}$ is the covariance at time T_k given only past observations, $\hat{\mathbf{P}}_{T_k}$ is the covariance at time T_k given additional observations between T_k and T_{k+1} .

By treating each $\mathbf{x}^*(T_k)$ as an initial condition with stage-wise observation time ΔT and applying Proposition IV.1, we obtain an EKF-like evolution for the prior and posterior covariances at each T_k :

$$\check{\mathbf{P}}_{T_{k+1}} = \Phi_{T_k, T_{k+1}} \hat{\mathbf{P}}_{T_k} \Phi_{T_k, T_{k+1}}^\top, \quad (35)$$

$$\hat{\mathbf{P}}_{T_k}^{-1} = \frac{\mathbf{W}_{\mathbf{R}-1}(\mathbf{x}^*(T_k), \mathbf{u} : [T_k, T_{k+1}] \rightarrow \mathcal{U})}{\Delta t} + \check{\mathbf{P}}_{T_k}^{-1}. \quad (36)$$

where $\Phi_{T_k, T_{k+1}} = D(\phi_{T_{k+1}} \phi_{T_k}^{-1})$ is the state transition map from time T_k to T_{k+1} .

We assume the inputs $\mathbf{u}(t)$ are *piecewise-constant* in each stage $[T_k, T_{k+1})$, so we can employ STLOG (IV.1) to approximate the full Gramian $\mathbf{W}_{\mathbf{R}-1}$ in (35).

Proposition V.1. *With assumptions as above, the prior and posterior covariances at stage- k are related in terms of the STLOG (IV.1) by*

$$\hat{\mathbf{P}}_{T_k}^{-1} = \frac{\mathbf{W}_{\mathbf{R}-1}^{(r)}(\mathbf{x}^*(T_k), \mathbf{u}(T_k))}{\Delta t} + \check{\mathbf{P}}_{T_k}^{-1}. \quad (37)$$

In particular, an analogous bound to (24) holds: The posterior precision due to the observations in $[T_k, T_{k+1})$ is bounded below by

$$\begin{aligned} & \lambda_{\max}^{-1}(\check{\mathbf{P}}_{T_k}) \\ & \geq \frac{\lambda_{\min}(\mathbf{W}_{\mathbf{R}-1}^{(r)}(\mathbf{x}^*(T_k), \mathbf{u}(T_k)))}{\Delta t} + \lambda_{\max}^{-1}(\check{\mathbf{P}}_{T_k}). \end{aligned} \quad (38)$$

In other words, the minimum eigenvalue of the STLOG in (38) provides a lower bound to the improvement in precision due to observations in $[T_k, T_{k+1})$.

Remark. The covariance update equation (37) becomes equivalent to the original EKF covariance update equation if we take $r = 0$ and $\Delta T/\Delta t = 1$. In this case, only a single observation is received in each stage and the effects of system dynamics are moot. This is reflected in the order-0 STLOG, which is expressed as $\mathbf{W}_{\mathbf{R}-1}^{(0)} = \Delta T \mathbf{H}^\top \mathbf{R}^{-1} \mathbf{H}$. Substituting this expression transforms (37) into the ubiquitous Kalman update law

$$\hat{\mathbf{P}}_{T_k}^{-1} = \mathbf{H}^\top \mathbf{R}^{-1} \mathbf{H} + \check{\mathbf{P}}_{T_k}^{-1}. \quad (39)$$

We propose that we maximize the sum of the minimum precision improvements along the trajectory, leading to the following principle:

Definition V.1 (Observability Aware Control). Solving the optimal control problem

$$\max_{\mathbf{u}(T_0, \dots, T_{N-1})} \sum_{k=0}^{N-1} \lambda_{\min}(\mathbf{W}_{\mathbf{R}-1}^{(r)}(\mathbf{x}^*(T_k), \mathbf{u}(T_k))), \quad (40)$$

subject to state dynamics (7) yields an observability-optimal sequence of control inputs $\mathbf{u}(t) = \mathbf{u}_k$ for $t \in [T_k, T_{k+1})$.

The principle (V.1) builds upon the fact that $\mathbf{W}_{\mathbf{R}-1}$ can be evaluated analytically. In this case, no numerical integration is involved inside the cost function (40).

A. Relationship with other metrics of observability

The proposed observability-aware control principle (V.1) is derived from a state estimation framework. Surprisingly, the principle (V.1) can be reconciled with the notions of observability introduced in Sec. IV-A.

Firstly, the discrete rank-testing notion of observability is recovered from the asymptotic behavior of the objective function (40). More precisely, the asymptotics of the summand $\lambda_{\min}(\mathbf{W}_{\mathbf{R}-1}^{(r)}(\mathbf{x}, \mathbf{u}; \Delta T))$ as $\Delta T \rightarrow 0$ *detects* the local observability index $r_*(\mathbf{x}, \mathbf{u})$ (10).

Proposition V.2. *With the notation above,*

- 1) *If $r < r_*(\mathbf{x}, \mathbf{u})$, then $\lambda_{\min}(\mathbf{W}_{\mathbf{R}-1}^{(r)}(\mathbf{x}, \mathbf{u}; \Delta T)) = 0$,*
- 2) *If $r \geq r_*(\mathbf{x}, \mathbf{u})$, then for all sufficiently small ΔT ,*

$$\lambda_{\min}(\mathbf{W}_{\mathbf{R}-1}^{(r)}(\mathbf{x}, \mathbf{u}; \Delta T)) = C(\mathbf{x}, \mathbf{u}; \Delta T) \Delta T^{2r_*+1}, \quad (41)$$

where $C(\mathbf{x}, \mathbf{u}; \Delta T)$ is bounded between two positive quantities C_1, C_2 depending only on (\mathbf{x}, \mathbf{u}) and not ΔT : $0 < C_1(\mathbf{x}, \mathbf{u}) \leq C \leq C_2(\mathbf{x}, \mathbf{u})$.

We defer the detailed proof to Appendix A.

Proposition V.2 suggests that, in the principle (40), stages yielding low $r_*(\mathbf{x}, \mathbf{u})$ make asymptotically larger contributions to the sum compared to stages yielding high $r_*(\mathbf{x}, \mathbf{u})$. Thus, observability-optimal trajectories obtained by solving (40) will avoid points with high r_* and favor regions where r_* attains the minimum value permitted by the dynamics (7)³.

Next, we consider metrics of observability.

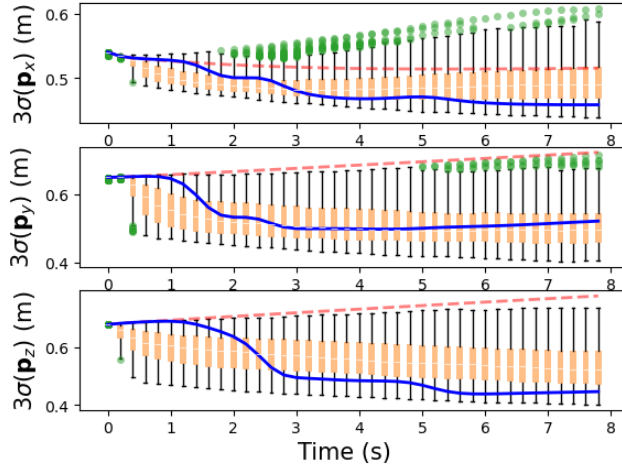
The constants C_1, C_2 in Proposition V.2 are shown to be (Propositions A.4 and A.7, Appendix A)

$$C_1 = \alpha \sigma_{\min}^2(\mathcal{O}^{(r_*)}), \quad (42)$$

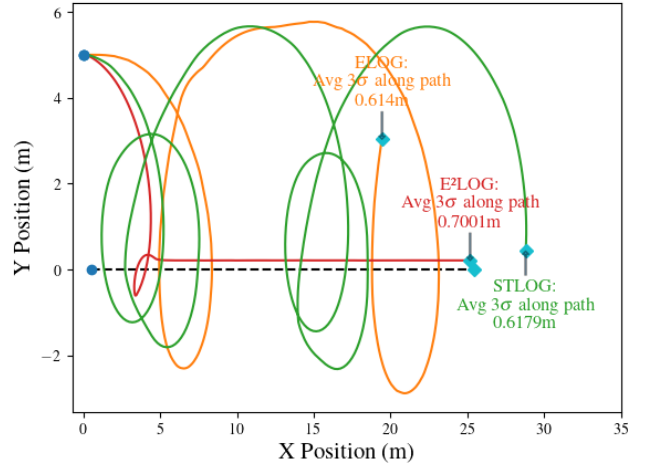
$$C_2 = \beta \sigma_{\min}^2(\mathcal{O}^{(r_*)}|_{\ker \mathcal{O}^{(r_*-1)}}), \quad (43)$$

where σ_{\min} denotes the minimum singular value of a matrix, $|$ denotes the restriction to a subspace, and α, β are numerical constants. C_1 and C_2 are metrics of observability based on the minimum singular value of the observability matrix [7], [8], with C_2 focusing on the previously unobservable subspace $\ker \mathcal{O}^{(r_*-1)}$. One can thus form a new metric of observability C' from some weighted average of C_1 and C_2 ,

³Dimension counting on the observability matrix $\mathcal{O}^{(r)}$ (9) shows that $r_*(\mathbf{x}, \mathbf{u}) \geq \lceil \dim \mathcal{X} / \dim \mathcal{Y} \rceil - 1$ for all (\mathbf{x}, \mathbf{u}) .



(a) Solving the Optimization Problem: Development of position estimation covariance along each axis over uniform (red), observability-optimal (green), and 1000 random (summarized by box plots) trajectories.



(b) Impact of Gramian approximator: Observability-Optimal trajectories for the follower computed using the ELOG (orange), E²LOG (red), and STLOG (green) while the leader flies on a straight (black dashed) path.

Fig. 3. Results from two rounds of simulations to evaluate the Observability-Aware Control Principle and the OPC

then heuristically approximate the function C in (41) with C' to obtain a control law

$$\max \sum_{k=0}^{N-1} C'(\mathbf{x}^*(T_k), \mathbf{u}(T_k)) \Delta T^{2r_*(\mathbf{x}^*(T_k), \mathbf{u}(T_k))+1}, \quad (44)$$

subject to state dynamics (7). For the same value of r_* , stages with a higher metric of observability C' will contribute more in the approximate principle (44), leading to observability-optimal trajectories from the dynamical systems' viewpoint under the metric C' .

VI. IMPLEMENTATION

A. Computation Of The STLOG

We use *automatic differentiation* to compute Lie Derivatives in the STLOG per (30), specifically using the `jax` [27] framework to evaluate pushforwards $(\mathbf{x}, \mathbf{v}) \mapsto (D\mathbf{f}(\mathbf{x}))\mathbf{v}$, to build up the Lie Derivative of any generic function.

We also use `jax`'s Just-In-Time (JIT) compilation feature to speed up the evaluation of the STLOG. The cost of evaluating the JIT-compiled STLOG is competitive with a symbolically derived alternative as shown in Table I.

TABLE I
BENCHMARK OF VARIOUS IMPLEMENTATIONS OF THE STLOG

Provider	<code>jax</code>	MATLAB
Diff Mode	Autodiff	Symbolic Algebra
Exec Mode	JIT compiled	Compiled, generated C code
Exec Time	$68.0\mu s \pm 858ns$	$55.8\mu s \pm 169ns$

Note: Timings reported as mean \pm std. dev. of 7 runs, 10000 loops each

However, support for `jax` on ARM-architected embedded computers commonly used onboard mobile robots is experimental to our best knowledge. Therefore, we designed our flight tests around this limitation by computing observability-optimal control strategies ahead of time.

B. Implementation of Observability-Aware Control

Solving the observability aware control problem given by Definition (V.1) in a receding-horizon manner gives rise to

Definition VI.1 (Observability-Predictive Controller).

$$\max_{\mathbf{u}_0, \dots, \mathbf{u}_{N-1}} \sum_{k=0}^{N-1} \log^{-1} \left(\lambda_{\min} \left(\mathbf{W}_{\mathbf{R}^{-1}}^{(r)}(\mathbf{x}_k^*, \mathbf{u}_k) \right) \right), \quad (45)$$

$$\mathbf{x}_k = \text{RK4}(\mathbf{f})(\mathbf{x}_{k-1}, \mathbf{u}_k), \quad \mathbf{x}_0 = \mathbf{x}_{\text{curr}}$$

$$\text{subject to } u_{\min, i} \leq \mathbf{u}_{k, i} \leq u_{\max, i} \quad (46)$$

$$g_{\min} \leq \mathbf{g}(\mathbf{x}_k, \mathbf{u}_k) \leq g_{\max}$$

where the reciprocal-of-logarithm mitigates scaling issues when the minimum eigenvalue becomes small.

In a CL context, the nonlinear constraint comprises bounds on the distance between each pair of vehicles

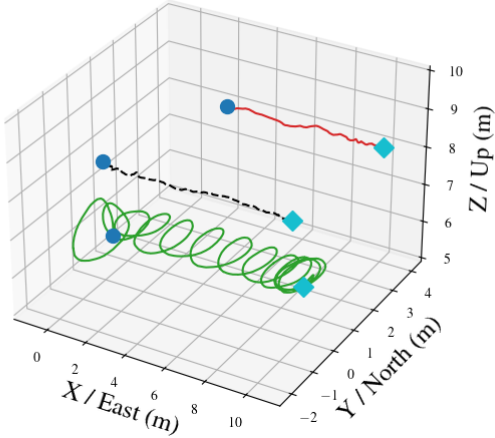
$$g_{\min} \leq \rho^{jk} \leq g_{\max} \quad \forall j, k \in \binom{N}{2} \quad (47)$$

Note. Equation (46) is consistent with the Model Predictive Controller (MPC) formalism. T becomes our prediction horizon and $T = N\Delta T$ the discretization scheme. This provides the basis for this controller to be executed in *real-time* once limitations mentioned in VI-A are lifted.

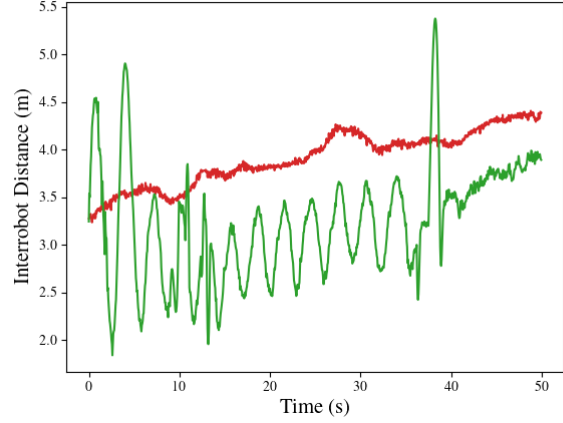
We use `scipy.optimize.minimize` to solve this problem, and we chose the `trust-constr` algorithm.

VII. EXPERIMENTAL VALIDATION

We verify our contributions in both simulations and experiments. Firstly, we verify the observability control principle and the STLOG that underlies in simulations. Secondly, we verify the benefits of using the STLOG instead of other Gramian approximation schemes. Subsequently, we experimentally verify the trajectories generated by the Observability Predictive Controller by executing them with quadrotors equipped with real Cooperative Localization hardware.



(a) Quadrotor trajectories in flight tests. The follower executes a straight (red) and an observability optimal (green) trajectory in two separate trials, while the leader travels along a straight (black dashed) path.



(b) Interrobot distance reported by the UWB system as the follower vehicle traveled along a straight (red) and an observability optimal (green) trajectory.

Fig. 4. Results from flight testing quadrotors equipped with a cooperative localization system

A. Simulation

1) *Solving the Optimization Problem:* We verify Principle V.1 in isolation by demonstrating that reasonably minimal state estimation covariance is achieved through maximizing observability, thus reflecting the optimality of the solution.

We consider a quadrotor team containing 1) one leader following a manually specified straight trajectory 2) one follower whose trajectory is computed by solving the problem (40).

In our scenario, the leader flies along a straight path and the follower starts from a level-flying state. We solve the observability-aware control problem over a *single* observation horizon of $T = 8s$ broken down into $N = 40$ steps, with an observation period of $\delta t = 0.05s$ at each step.

For comparison, we generate 1) A uniform and straight trajectory that is *suboptimal* 2) 1000 random trajectories by sampling the input space within upper and lower bounds for the follower quadrotor.

Finally, we iterate the EKF covariance propagation over all aforementioned trajectories while recording the covariance in position estimation, which is graphed in Figure 3a. The positioning covariance along the observability-optimal trajectory is lower than the that along a majority of random trajectories (up to three quartiles) on the X and Z axes, and substantially lower than the positioning covariance along the straight trajectory in all cases. Thus, the observability-optimal trajectory is relatively optimal in the sense of covariance reduction, even when the optimum is clearly *local*.

2) *Impact of Gramian approximator:* We compute several quadrotor trajectories, using the Controller VI.1 to solve (40) *repeatedly* in a receding horizon framework, while the underlying Gramian approximation is varied between 1) Krener and Ide's ELOG; 2) Hausman and Priess's E²LOG; and 3) Our

STLOG.⁴

We reuse the scenario from the last simulation, but we restrict the quadrotors to maintain the same altitude for some reasons to be expanded, and to emphasize the geometry of the resultant trajectories, which are plotted in Figure 3b.

When the STLOG is used to approximate the Gramian in the observability-optimal control problem, the solution lets the follower quadrotor exhibit an 'orbiting' behavior that complies with observability-optimal behavior shown in [25],

However, when the E²LOG is used, the optimizer hit a point that thwarted its ability to obtain any meaningful solution, after which the follower settles into a straight path — shown to be suboptimal previously — and yielding the highest positioning covariance of 0.7001 m along which. True to Point 2 under Remark IV-C, this phenomenon is exacerbated when we reduced the stepsize Δt further below 0.05s. On the other hand, this phenomenon is alleviated by allowing altitude variation, corroborating the loss of state-transition information from the E²LOG as $\Delta t \rightarrow 0$, which is ameliorated by complex, three-dimensional motion.

When the ELOG is used, the solution trajectory is outwardly similar to that obtained using the STLOG, and the covariance yielded is even marginally better (0.6179 m) to that along the STLOG-optimal trajectory (0.614 m). This comes at the cost of very significant computational time (more than 4 times longer per solver iteration compared to when ELOG/STLOG are used) due to the numerically-integrated nature of the ELOG, which is only mitigated here by forbidding altitude variation.

B. Quadrotor Flight Experiments

Next, we apply our Controller (OPC) VI.1 to controlling quadrotors, described in Table II, in a scenario that builds

⁴The $\{E, E^2\}$ LOG are not designed to be evaluated point-wise, but we retrofit them to a receding-horizon framework by evaluating **one** $\{E, E^2\}$ LOG over each predictive horizon then taking their minimum eigenvalue as the cost value, instead of evaluating running cost at each point

upon the leader-follower quadrotor team of our simulations.

TABLE II
CONFIGURATION OF QUADROTOR EXPERIMENTAL PLATFORMS

Type	Name and Specifications
Airframe	F450 (1.7 kg, 5" props, 4500mAh LiPo)
Autopilot	Cube Orange (PX4 1.14.5)
Onboard Computer	Jetson TX2 NX (JetPack 4.6)
GNSS unit (leader)	UBlox M8N
UWB unit (follower)	ESP32 UWB DWM3000

Following the simulation procedure, we require the leader quadrotor to fly along a straight path, and the follower quadrotor executes 1) A suboptimal uniform trajectory 2) An observability-optimal trajectory in two separate trials.

Per Subsection VI-A, we compute the observability-optimal trajectory for case 2 ahead-of-time on a ground station and transmit it to airborne quadrotors in the form of a sequence (trajectory) of timestamped states and inputs.

In this process, the solver successfully solved the underlying optimal control problem on every invocation. Table III shows the computational results of 2000 invocations of the solver, one per timestep, collected during these two cases.

TABLE III
STATISTICS OF COMPUTATIONAL OPTIMIZATION RESULTS OVER ALL RUNS

Parameter	Value		
	Min	Max	Mean
Δ Objective	1.56e-06	0.0749	0.00929 \pm 0.00649
# Solver Iters	42	150	49.6 \pm 7.64
Exec Time (s)	1.74	15.4	2.92 \pm 0.765
Optimality	0.00161	0.0798	0.00823 \pm 0.00439

During flight tests, a cooperative localization system based on our formulation in [19] concurrently runs to offer position estimates for the quadrotor team. We assess the 3σ — three standard deviations — value in positioning reported by this system. Figure 5 displays the state estimation performance recorded during the simulation.

In both flight tests, the standard deviation in the positioning of the follower quadrotor is always under 2 meters, driving home our belief since our previous studies that cooperative localization is competitive with GNSS. Then, observability-optimal trajectories contributed to substantially higher positioning confidence on the x-axis, with the RMS of the positioning standard deviation being 0.46 m, close to half a meter lower, than that obtained along uniform trajectories. This phenomenon is even more pronounced on the z-axis, with positioning being more than twice as confident along observability-optimal trajectories than along uniform trajectories.

As for the overall behavior of the system, we inspect the trajectories, executed by the quadrotor team, shown in Figure 4a. The distinctive ‘orbiting’ behavior is reproduced, which is also consistent with the undulating positioning covariance

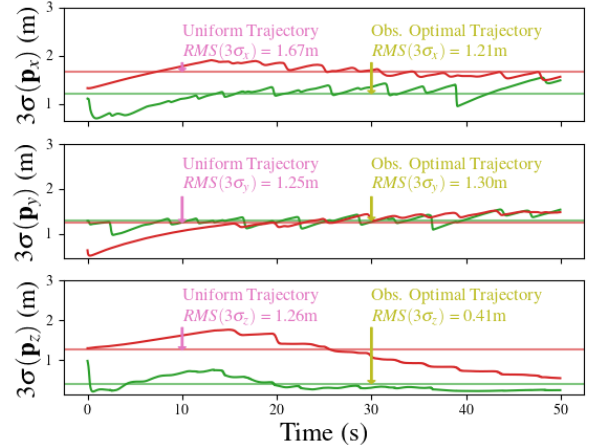


Fig. 5. Positioning standard deviation recorded on the follower quadrotor (cooperative localizing) during flight tests, when performing uniform trajectories (orange) and observability-optimal trajectories (green)

along the observability-optimal trajectory in Figure 5. This indicates that the OPC is in a cycle of maintaining an acceptable interrobot distance and seeking maximal observability, a feat not achievable with traditional controllers that seek a rigid formation or steady, non-oscillatory trajectories. On the other hand, Figure 4b showed that the interrobot range measurement oscillated periodically as the follower traveled along observability-optimal trajectories. This also corroborates the pattern of range measurement analytically proven in [25] to yield maximum observability.

VIII. CONCLUSION

We have proposed an Observability-Aware Controller based on the STLOG, a novel approximation of the Observability Gramian that respects the goal of reducing state estimation covariance. We applied this controller to the problem of cooperative localization of quadrotors, and showcased the efficacy of this controller in numerical simulations. Then, after developing a UWB-based interrobot ranging system, we deployed our controller in flight tests.

We took an integrated approach in experimentally verifying our work. As such, there is room for experiments at a finer granularity. For example, more introspection could be done on the structure of our control Problem and the quality of solutions. More intensive experiments can be done to assess the state estimation performance — not just covariance but also error — along observability-optimal trajectories. Similarly, more experiments can be done to compare our controller to alternative cooperative control strategies.

We envision further work as suggested above would bring key insights to simplify observability-optimal control problem or relieve the computational burden of solving it, contributing to solving the remaining open problem of running observability-aware controllers in real-time on mobile robots.

ACKNOWLEDGEMENTS

We would like to acknowledge the sponsorship by the Natural Sciences and Engineering Research Council of Canada (NSERC) under grant RGPIN-2023-05148. We would also like to acknowledge our summer student, Tommy Zhang, for contributing to flight testing and hardware interfacing of quadrotor platforms.

APPENDIX

APPENDIX A

ASYMPTOTIC SIZE OF THE MINIMUM EIGENVALUE OF THE SHORT-TERM LOCAL OBSERVABILITY GRAMIAN

This Appendix is concerned with the derivation of Proposition V.2. This asymptotic result relates the short-term local observability Gramian (IV.1) to the local observability index r_* (10) from rank-testing observability. Throughout the section, we fix a single (\mathbf{x}, \mathbf{u}) .

We make a number of inessential assumptions to simplify the notation and the proof. We set the observation covariance $\mathbf{R} = \mathbf{1}$, and drop the subscript \mathbf{R}^{-1} from the STLOG (IV.1) and simply denote the order- r STLOG by $\mathbf{W}^{(r)}$.

The main result of this appendix concerns the asymptotic size of $\lambda_{\min}(\mathbf{W}^{(r)}(\mathbf{x}, \mathbf{u}; \Delta T))$ as $\Delta T \rightarrow 0$. We show that the local observability index $r_*(\mathbf{x}, \mathbf{u})$ emerges in the limit.

Theorem A.1. *Let (\mathbf{x}, \mathbf{u}) be given and $r_*(\mathbf{x}, \mathbf{u})$ be its local observability index. Consider the minimum eigenvalue of the order- r STLOG $\mathbf{W}^{(r)}(\mathbf{x}, \mathbf{u}; \Delta T)$.*

- 1) If $r < r_*(\mathbf{x}, \mathbf{u})$, then $\lambda_{\min}(\mathbf{W}^{(r)}(\mathbf{x}, \mathbf{u}; \Delta T)) = 0$.
- 2) If $r \geq r_*(\mathbf{x}, \mathbf{u})$, then for all sufficiently small ΔT , there exists positive constants $C_1(\mathbf{x}, \mathbf{u}), C_2(\mathbf{x}, \mathbf{u})$ independent of ΔT such that

$$C_1(\mathbf{x}, \mathbf{u})\Delta T^{2r_*(\mathbf{x}, \mathbf{u})+1} \leq \lambda_{\min}(\mathbf{W}^{(r)}(\mathbf{x}, \mathbf{u}; \Delta T)) \leq C_2(\mathbf{x}, \mathbf{u})\Delta T^{2r_*(\mathbf{x}, \mathbf{u})+1}. \quad (48)$$

In particular, there exists some $C \in [C_1, C_2]$ and a sequence $\Delta T_k \rightarrow 0$ such that

$$\lim_{k \rightarrow \infty} \frac{\lambda_{\min}(\mathbf{W}^{(r)}(\mathbf{x}, \mathbf{u}; \Delta T_k))}{\Delta T_k^{2r_*(\mathbf{x}, \mathbf{u})+1}} = C. \quad (49)$$

We prove part (1) through rank considerations and part (2) by explicitly constructing the upper and lower bounds.

We say the system is *locally observable at order r* if $\text{rank } \mathcal{O}^{(r)} = \dim \mathcal{X}$. Consider the following subspaces

$$\mathcal{H}_k = \bigcap_{i=0}^k \ker(DL_{\mathbf{f}}^i \mathbf{h}) = \ker \mathcal{O}^{(k)}. \quad (50)$$

Clearly, $\mathcal{H}_{k-1} \supset \mathcal{H}_k$. This decreasing sequence of subspaces reaches $\{0\}$ precisely at the local observability index r_* .

Lemma A.2.

- 1) $\mathcal{H}_r = \{0\} \Leftrightarrow$ the system is locally observable at order r .
- 2) The local observability index $r_*(\mathbf{x}, \mathbf{u})$ is the smallest value of r such that $\mathcal{H}_r = \{0\}$.
- 3) In particular, if $r_* > 0$, then \mathcal{H}_{r_*-1} is nonzero.

We rewrite the STLOG (IV.1) in terms of the observability matrix before evaluating the integral (17). For any $\mathbf{v}, \tilde{\mathbf{v}} \in \mathcal{X}$,⁵

$$\mathbf{v}^\top \mathbf{W}^{(r)} \tilde{\mathbf{v}} = \int_0^{\Delta T} \left\langle \begin{bmatrix} \mathbf{1} & t\mathbf{1} & \cdots & \frac{t^r}{r!}\mathbf{1} \end{bmatrix} \mathcal{O}^{(r)} \mathbf{v}, \begin{bmatrix} \mathbf{1} & t\mathbf{1} & \cdots & \frac{t^r}{r!}\mathbf{1} \end{bmatrix} \mathcal{O}^{(r)} \tilde{\mathbf{v}} \right\rangle dt, \quad (51)$$

which makes $\mathbf{W}^{(r)}$ manifestly positive semi-definite. The positive-definiteness of $\mathbf{W}^{(r)}$ is linked to local observability:

Proposition A.3. *The system is not locally observable at order $r \Leftrightarrow \lambda_{\min}(\mathbf{W}^{(r)}) = 0$.*

This implies part (1) of Theorem A.1.

Proof. Suppose the system is not locally observable at order r . By Lemma (A.2), there exists some nonzero $\mathbf{v} \in \mathcal{H}_r$. In particular, $\mathcal{O}^{(r)} \mathbf{v} = 0$. Substituting into (51) gives $\mathbf{v}^\top \mathbf{W}^{(r)} \mathbf{v} = 0$, so $\lambda_{\min}(\mathbf{W}^{(r)}) = 0$.

Conversely, suppose $\lambda_{\min}(\mathbf{W}^{(r)}) = 0$. Then there exists some nonzero $\mathbf{v} \in \mathcal{X}$ such that $\mathbf{v}^\top \mathbf{W}^{(r)} \mathbf{v} = 0$. Using (51):

$$\int_0^{\Delta T} \left\| \begin{bmatrix} \mathbf{1} & t\mathbf{1} & \cdots & \frac{t^r}{r!}\mathbf{1} \end{bmatrix} \mathcal{O}^{(r)} \mathbf{v} \right\|^2 dt = 0, \quad (52)$$

from which we deduce

$$\begin{bmatrix} \mathbf{1} & t\mathbf{1} & \cdots & \frac{t^r}{r!}\mathbf{1} \end{bmatrix} \mathcal{O}^{(r)} \mathbf{v} = 0, \quad \forall t \in [0, \Delta T], \quad (53)$$

which implies $\mathcal{O}^{(r)} \mathbf{v} = 0$, so the system is not locally observable at order r . \square

Next, we prove the upper and lower bounds in part (2) of Theorem A.1. Let r_* be the local observability index. We only consider $\mathbf{W}^{(r)}$ with $r \geq r_*$ in the following, and assume $r_* > 0$ without loss of generality.

We first prove the upper bound. Recall that

$$\lambda_{\min}(\mathbf{W}^{(r)}) = \min_{\mathbf{v} \in \mathcal{X}, \|\mathbf{v}\|=1} \mathbf{v}^\top \mathbf{W}^{(r)} \mathbf{v}. \quad (54)$$

We thus seek an appropriate unit vector \mathbf{v} that demonstrates the upper bound in (A.1). Any unit vector $\mathbf{v} \in \mathcal{H}_{r_*-1}$ satisfies

$$(DL_{\mathbf{f}}^{r_*} \mathbf{h}) \mathbf{v} \neq 0, \quad (DL_{\mathbf{f}}^k \mathbf{h}) \mathbf{v} = 0 \text{ for all } k < r_*. \quad (55)$$

In particular, $\|(DL_{\mathbf{f}}^{r_*} \mathbf{h}) \mathbf{v}\| = \|\mathcal{O}^{(r_*)} \mathbf{v}\|$. Pick a unit vector \mathbf{v} that minimizes $\|(DL_{\mathbf{f}}^{r_*} \mathbf{h}) \mathbf{v}\|$. For such \mathbf{v} , we have

$$\|(DL_{\mathbf{f}}^{r_*} \mathbf{h}) \mathbf{v}\| = \sigma_{\min}(\mathcal{O}^{(r_*)}|_{\mathcal{H}_{r_*-1}}) > 0, \quad (56)$$

where $|_{\mathcal{H}_{r_*-1}}$ denotes the restriction to the subspace \mathcal{H}_{r_*-1} .

Now we evaluate $\mathbf{v}^\top \mathbf{W}^{(r)} \mathbf{v}$ using our \mathbf{v} (55), (56). Firstly,

$$\begin{aligned} & \begin{bmatrix} \mathbf{1} & t\mathbf{1} & \cdots & \frac{t^r}{r!}\mathbf{1} \end{bmatrix} \mathcal{O}^{(r)} \mathbf{v} \\ &= \frac{t^{r_*}}{r_*!} (DL_{\mathbf{f}}^{r_*} \mathbf{h}) \mathbf{v} + t^{r_*+1} \mathbf{a}(\mathbf{v}, t), \end{aligned} \quad (57)$$

for some polynomial $\mathbf{a}(\mathbf{v}, t)$. Substituting (57) into (51) and integrating gives

$$\begin{aligned} & \mathbf{v}^\top \mathbf{W}^{(r)} \mathbf{v} \\ &= \frac{\Delta T^{2r_*+1} \|(DL_{\mathbf{f}}^{r_*} \mathbf{h}) \mathbf{v}\|^2}{(r_*!)^2 (2r_*+1)} + \Delta T^{2r_*+2} \alpha(\mathbf{v}, \Delta T), \end{aligned} \quad (58)$$

⁵In (51), if instead of the standard inner product on \mathcal{Y} we use the inner product induced by \mathbf{R}^{-1} , we recover the expressions (17), (IV.1).

for some polynomial $\alpha(\mathbf{v}, \Delta T)$.

Let $|\alpha(\mathbf{v}, \Delta T)| \leq A$ for all sufficiently small ΔT and all unit vectors \mathbf{v} , and $B = \frac{\sigma_{\min}^2(\mathcal{O}^{(r_*)} |_{\mathcal{H}_{r_*-1}})}{(r_*!)^2(2r_*+1)}$. We have:

$$\lambda_{\min}(\mathbf{W}^{(r)}) \leq \mathbf{v}^\top \mathbf{W}^{(r)} \mathbf{v} \leq \Delta T^{2r_*+1} (B + A\Delta T). \quad (59)$$

For any $\epsilon > 0$, choosing $\Delta T < \epsilon B/A$ gives:

Proposition A.4. *For all $\epsilon > 0$, there exists $\delta > 0$ such that*

$$\lambda_{\min}(\mathbf{W}^{(r)}) \leq \frac{(1 + \epsilon)\Delta T^{2r_*+1}\sigma_{\min}^2(\mathcal{O}^{(r_*)} |_{\mathcal{H}_{r_*-1}})}{(r_*!)^2(2r_*+1)}, \quad (60)$$

for all $\Delta T < \delta$.

Next we prove the lower bound in (48). It is convenient to rewrite the STLOG (IV.1) into block matrix form

$$\mathbf{W}^{(r)} = \Delta T \mathcal{O}^{(r)\top} \mathbf{\Lambda}^{(r)} \mathcal{H}^{(r)} \mathbf{\Lambda}^{(r)} \mathcal{O}^{(r)}, \quad (61)$$

where $\mathbf{\Lambda}^{(r)}$ is the block diagonal matrix

$$\mathbf{\Lambda}^{(r)} = \text{diag} \left(\mathbf{1} \quad \Delta T \mathbf{1} \quad \dots \quad \frac{\Delta T^r}{r!} \mathbf{1} \right), \quad (62)$$

and $\mathcal{H}^{(r)}$ is the block matrix whose entries correspond to a finite-order Hilbert matrix [28], [29]:

$$\mathcal{H}^{(r)} = \begin{bmatrix} \mathbf{1} & \frac{1}{2}\mathbf{1} & \dots & \frac{1}{r}\mathbf{1} \\ \frac{1}{2}\mathbf{1} & \frac{1}{3}\mathbf{1} & \dots & \frac{1}{r+1}\mathbf{1} \\ \vdots & \vdots & \ddots & \vdots \\ \frac{1}{r}\mathbf{1} & \frac{1}{r+1}\mathbf{1} & \dots & \frac{1}{2r+1}\mathbf{1} \end{bmatrix}. \quad (63)$$

It is well-known [28], [29] that the Hilbert matrix $\mathcal{H}^{(r)}$ for each r is positive definite. This allows us to prove the lower bound in (48) with a lower bound on $\mathbf{\Lambda}^{(r)} \mathcal{O}^{(r)} \mathbf{v}$.

Lemma A.5. *Let $\mathbf{v} \in \mathcal{X}$ be a unit vector. Then for $\Delta T \leq 1$,*

$$\left\| \mathbf{\Lambda}^{(k)} \mathcal{O}^{(k)} \mathbf{v} \right\| \geq \frac{\Delta T^k}{k!} \sigma_{\min}(\mathcal{O}^{(k)}). \quad (64)$$

Proof. By substituting the value of $\sigma_{\min}(\mathbf{\Lambda}^{(r)})$ from (62) and $\|\mathbf{v}\| = 1$ in the last step, we get

$$\begin{aligned} \left\| \mathbf{\Lambda}^{(k)} \mathcal{O}^{(k)} \mathbf{v} \right\| &\geq \sigma_{\min}(\mathbf{\Lambda}^{(k)} \mathcal{O}^{(k)}) \|\mathbf{v}\| \\ &\geq \sigma_{\min}(\mathbf{\Lambda}^{(k)}) \sigma_{\min}(\mathcal{O}^{(k)}) \|\mathbf{v}\| = \frac{\Delta T^k}{k!} \sigma_{\min}(\mathcal{O}^{(k)}), \end{aligned} \quad \square$$

The bound (64) admits a straightforward but important improvement for $r \geq r_*$:

Lemma A.6. *Let $\mathbf{v} \in \mathcal{X}$ be a unit vector, and let $r \geq r_*$. Then for $\Delta T \leq 1$,*

$$\left\| \mathbf{\Lambda}^{(r)} \mathcal{O}^{(r)} \mathbf{v} \right\| \geq \frac{\Delta T^{r_*}}{r_*!} \sigma_{\min}(\mathcal{O}^{(r_*)}), \quad (65)$$

where $\sigma_{\min}(\mathcal{O}^{(r_*)})$ is positive and independent of ΔT .

Proof. Write the vector $\mathbf{\Lambda}^{(r)} \mathcal{O}^{(r)} \mathbf{v}$ as a block of two vectors

$$\mathbf{\Lambda}^{(r)} \mathcal{O}^{(r)} \mathbf{v} = \begin{bmatrix} \mathbf{\Lambda}^{(r_*)} \mathcal{O}^{(r_*)} \mathbf{v} \\ \mathbf{w} \end{bmatrix},$$

where \mathbf{w} is a $(r - r_*) \dim \mathcal{Y} \times 1$ column vector. Now

$$\begin{aligned} \left\| \mathbf{\Lambda}^{(r)} \mathcal{O}^{(r)} \mathbf{v} \right\| &= \sqrt{\left\| \mathbf{\Lambda}^{(r_*)} \mathcal{O}^{(r_*)} \mathbf{v} \right\|^2 + \|\mathbf{w}\|^2} \\ &\geq \left\| \mathbf{\Lambda}^{(r_*)} \mathcal{O}^{(r_*)} \mathbf{v} \right\| \geq \frac{\Delta T^{r_*}}{r_*!} \sigma_{\min}(\mathcal{O}^{(r_*)}), \end{aligned}$$

where we used the bound (64) for $k = r_*$ in the last step. \square

Proposition A.7. *For all $\Delta T \leq 1$, we have*

$$\lambda_{\min}(\mathbf{W}^{(r)}) \geq \frac{a^{(r)} \Delta T^{2r_*+1} \sigma_{\min}^2(\mathcal{O}^{(r_*)})}{(r_*!)^2}, \quad (66)$$

where $a^{(r)} > 0$ is the minimum eigenvalue of the Hilbert matrix of order r (63).

Proof. Let \mathbf{v} be any unit vector in \mathcal{X} . Using (61), we rewrite $\mathbf{v}^\top \mathbf{W}^{(r)} \mathbf{v}$ as

$$\mathbf{v}^\top \mathbf{W}^{(r)} \mathbf{v} = \Delta T \langle \mathcal{H}^{(r)} \mathbf{\Lambda}^{(r)} \mathcal{O}^{(r)} \mathbf{v}, \mathbf{\Lambda}^{(r)} \mathcal{O}^{(r)} \mathbf{v} \rangle, \quad (67)$$

where $\mathcal{H}^{(r)}$ is the Hilbert matrix (63). Therefore,

$$\begin{aligned} \mathbf{v}^\top \mathbf{W}^{(r)} \mathbf{v} &\geq \Delta T a^{(r)} \left\| \mathbf{\Lambda}^{(r)} \mathcal{O}^{(r)} \mathbf{v} \right\|^2 \\ &\geq \Delta T a^{(r)} \left(\frac{\Delta T^{r_*}}{r_*!} \sigma_{\min}(\mathcal{O}^{(r_*)}) \right)^2, \end{aligned}$$

using (65) in the last step. Simplifying and minimizing over unit vectors $\mathbf{v} \in \mathcal{X}$ gives the inequality (66). \square

Combining Propositions A.4, A.7, we have, for all sufficiently small ΔT ,

$$\alpha \sigma_{\min}^2(\mathcal{O}^{(r_*)}) \leq \frac{\lambda_{\min}(\mathbf{W}^{(r)})}{\Delta T^{2r_*+1}} \leq \beta \sigma_{\min}^2(\mathcal{O}^{(r_*)} |_{\mathcal{H}_{r_*-1}}), \quad (68)$$

where α, β are constants. Thus, we proved the inequality (48) in Theorem A.1 by explicitly constructing $C_1(\mathbf{x}, \mathbf{u}), C_2(\mathbf{x}, \mathbf{u})$ in terms of $\mathcal{O}^{(r_*)}$ only. The last part of Theorem A.1 follows from the Bolzano—Weierstrass theorem.

REFERENCES

- [1] Ioannis M Rekleitis, Gregory Dudek, and Evangelos E Milios. “Multi-robot exploration of an unknown environment, efficiently reducing the odometry error”. In: *International joint conference on artificial intelligence*. Vol. 15. LAWRENCE ERLBAUM ASSOCIATES LTD. 1997, pp. 1340–1345.
- [2] Ioannis Rekleitis, Gregory Dudek, and Evangelos Milios. “Multi-robot collaboration for robust exploration”. In: *Annals of Mathematics and Artificial Intelligence* 31 (2001), pp. 7–40.
- [3] Stergios I Roumeliotis and George A Bekey. “Distributed multirobot localization”. In: *IEEE transactions on robotics and automation* 18.5 (2002), pp. 781–795.
- [4] Yaohong Qu and Youmin Zhang. “Cooperative localization against GPS signal loss in multiple UAVs flight”. In: *Journal of Systems Engineering and Electronics* 22.1 (2011), pp. 103–112.

- [5] Amedeo Rodi Vetrella, Roberto Opromolla, Giancarmine Fasano, et al. “Autonomous flight in GPS-challenging environments exploiting multi-UAV cooperation and vision-aided navigation”. In: *AIAA Information Systems-AIAA Infotech Aerospace*. 2017, p. 0879.
- [6] Flavia Causa, Amedeo Rodi Vetrella, Giancarmine Fasano, et al. “Multi-UAV formation geometries for cooperative navigation in GNSS-challenging environments”. In: *2018 IEEE/ION position, location and navigation symposium (PLANS)*. 2018, pp. 775–785.
- [7] Arthur J Krener and Kayo Ide. “Measures of unobservability”. In: *Proceedings of the 48th IEEE Conference on Decision and Control (CDC) held jointly with 2009 28th Chinese Control Conference*. IEEE. 2009, pp. 6401–6406.
- [8] Karol Hausman, James Preiss, Gaurav S Sukhatme, et al. “Observability-aware trajectory optimization for self-calibration with application to uavs”. In: *IEEE Robotics and Automation Letters* 2.3 (2017), pp. 1770–1777.
- [9] James A Preiss, Karol Hausman, Gaurav S Sukhatme, et al. “Simultaneous self-calibration and navigation using trajectory optimization”. In: *The International Journal of Robotics Research* 37.13-14 (2018), pp. 1573–1594.
- [10] Christopher Grebe, Emmett Wise, and Jonathan Kelly. “Observability-aware trajectory optimization: Theory, viability, and state of the art”. In: *2021 IEEE International Conference on Multisensor Fusion and Integration for Intelligent Systems (MFI)*. IEEE. 2021, pp. 1–8.
- [11] Nikolas Trawny and Timothy Barfoot. “Optimized motion strategies for cooperative localization of mobile robots”. In: *IEEE International Conference on Robotics and Automation, 2004. Proceedings. ICRA’04. 2004. Vol. 1*. IEEE. 2004, pp. 1027–1032.
- [12] Yukikazu S Hidaka, Anastasios I Mourikis, and Stergios I Roumeliotis. “Optimal formations for cooperative localization of mobile robots”. In: *Proceedings of the 2005 IEEE International Conference on Robotics and Automation*. IEEE. 2005, pp. 4126–4131.
- [13] Xun S Zhou, Ke X Zhou, and Stergios I Roumeliotis. “Optimized motion strategies for localization in leader-follower formations”. In: *2011 IEEE/RSJ International Conference on Intelligent Robots and Systems*. IEEE. 2011, pp. 98–105.
- [14] Yongkyu Song and Jessy W Grizzle. “The extended Kalman filter as a local asymptotic observer for nonlinear discrete-time systems”. In: *1992 American control conference*. IEEE. 1992, pp. 3365–3369.
- [15] Konrad Reif, Stefan Gunther, Engin Yaz, et al. “Stochastic stability of the discrete-time extended Kalman filter”. In: *IEEE Transactions on Automatic control* 44.4 (1999), pp. 714–728.
- [16] Robert Hermann and Arthur Krener. “Nonlinear controllability and observability”. In: *IEEE Transactions on automatic control* 22.5 (1977), pp. 728–740.
- [17] Liang Zhang, Zexu Zhang, Roland Siegwart, et al. “A connectivity-prediction algorithm and its application in active cooperative localization for multi-robot systems”. In: *2020 IEEE International Conference on Robotics and Automation (ICRA)*. IEEE. 2020, pp. 9824–9830.
- [18] Alan Papalía, Nicole Thumma, and John Leonard. “Prioritized Planning for Cooperative Range-Only Localization in Multi-Robot Networks”. In: *2022 International Conference on Robotics and Automation (ICRA)*. IEEE. 2022, pp. 10753–10759.
- [19] HS Helson Go and Hugh H-T Liu. “Trajectory Optimization for Cooperatively Localizing Quadrotor UAVs”. In: *2024 IEEE International Conference on Robotics and Automation (ICRA)*. IEEE. 2024, pp. 11796–11803.
- [20] Rajnikant Sharma and Clark Taylor. “Cooperative navigation of MAVs in GPS denied areas”. In: *2008 IEEE International Conference on Multisensor Fusion and Integration for Intelligent Systems*. IEEE. 2008, pp. 481–486.
- [21] Anusna Chakraborty, Clark N Taylor, Rajnikant Sharma, et al. “Cooperative localization for fixed wing unmanned aerial vehicles”. In: *2016 IEEE/ION Position, Location and Navigation Symposium (PLANS)*. IEEE. 2016, pp. 106–117.
- [22] Anusna Chakraborty, Rajnikant Sharma, and Kevin Brink. “Cooperative localization for multi-rotor UAVs”. In: *AIAA Scitech 2019 Forum*. 2019, p. 0684.
- [23] Thomas Kailath. *Linear systems*. Vol. 156. Prentice-Hall Englewood Cliffs, NJ, 1980.
- [24] Kristoffer M Frey, Ted J Steiner, and Jonathan P How. “Towards online observability-aware trajectory optimization for landmark-based estimators”. In: *arXiv preprint arXiv:1908.03790* (2019).
- [25] Rohith Boyinine, Rajnikant Sharma, and Kevin Brink. “Observability based path planning for multi-agent systems to aid relative pose estimation”. In: *2022 International Conference on Unmanned Aircraft Systems (ICUAS)*. IEEE. 2022, pp. 912–921.
- [26] L.W. Tu. *An Introduction to Manifolds*. Second Edition. Springer New York, 2010. ISBN: 9781441973993.
- [27] James Bradbury, Roy Frostig, Peter Hawkins, et al. *JAX: composable transformations of Python+NumPy programs*. Version 0.3.13. 2018. URL: <http://github.com/google/jax>.
- [28] Man-Duen Choi. “Tricks or treats with the Hilbert matrix”. In: *The American Mathematical Monthly* 90.5 (1983), pp. 301–312.
- [29] John Todd. “Computational problems concerning the Hilbert matrix”. In: *J. Res. Nat. Bur. Standards Sect. B* 65 (1961), pp. 19–22.